Three-Body Bound States of Quantum Particles: Higher Stability Through Braiding

Sophie Fisher, Olumakinde Ogunnaike, Leonid Levitov
Massachusetts Institute of Technology, Cambridge, Massachusetts 02139, USA
(Dated: December 25, 2019)

Cold atoms embedded in a degenerate Fermi system interact by a fermionic analog of the Casimir force, in which the fermions play the role of photons. The fermion-mediated RKKY interaction is an attraction of a $-1/r$ form at distances shorter than the Fermi wavelength. While under realistic conditions the interaction strength is too weak to support hydrogenic two-particle bound states, the three-body bound states can have a considerably higher degree of stability. As a result, the trimer bound states can form even when the dimer states are unstable. We analyze three-body states associated with "figure-eight" periodic orbits of the classical problem and show that they are more stable than those associated with circular orbits. The spectra of resonances associated with the discrete energies of these states bear distinct signatures of the figure-eight braiding dynamics.

I. INTRODUCTION

One of the remarkable predictions of quantum theory is that when the interactions between particles are not strong enough to support a two-body bound state, they may nonetheless support three-body bound states. A celebrated example of this interesting behavior is Efimov trimers formed by particles interacting through short-range attractive interactions that are nearly resonant[1,2]. In this case, the three-body bound states, which form even though the two-body bound states are unstable, have a peculiar nested shell structure related to "discrete scale invariance" and limit cycles in the renormalization group[3–5]. These and other interesting properties have been a focus of active research in nuclear and cold atom physics, culminating in recent observations of a hierarchy of Efimov states in cold atom systems[6–8].

Cold atom systems also provide a unique platform to investigate other interesting few-body states. Here we discuss bound states of two and three bosonic particles embedded in a degenerate Fermi sea of cold atoms. A fermion-mediated interaction in this case arises through the so-called RKKY mechanism[9–11], illustrated in Fig.1 (a). The RKKY interaction takes the form

$$U(R) = -3\alpha \frac{\sin(2k_F R) - 2k_F R\cos(2k_F R)}{R^4}, \quad (1)$$

where k_F is the Fermi momentum, and the interaction strength α depends on the boson-fermion scattering length and particle masses, as discussed below. The fermion-mediated RKKY interaction between bosonic atoms was demonstrated in recent experiments with Bose-Einstein condensate of caesium atoms embedded in a degenerate Fermi gas of lithium atoms[12]. Interestingly, this interaction is a $1/r$ power-law at short distances:

$$U(R) = -\frac{\alpha}{R}, \quad 2k_F R < 1. \quad (2)$$

The power-law character of interaction at $2k_F R < 1$ and its sign (attraction) can be interpreted as a fermionic Casimir effect. The Casimir interaction between two bodies (or, atoms) arises due to scattering of virtual photons. For each of the bodies, angular distribution of the flux of incident virtual photons is somewhat anisotropic due to the presence of a second body, giving rise to a net attraction force. For fermionic paticles, this is illustrated in Fig.1 (a). The fermionic Casimir effect was also analyzed in other condensed matter systems[13].

Naturally, the behavior $U(R) \sim -1/R$ prompts the question of whether the two-particle bound states of a hydrogenic type, pictured schematically in Fig.1 (b), can occur. We argue below that, while the interaction strength α can be tuned by varying the fermion density and the boson-fermion scattering length, under realistic conditions it is too weak to support the two-body bound states. However, we find that the requirements for the formation of three-body bound states are not as stringent; and such states can indeed occur under realistic conditions.

As we will see, the three-body states originating from the RKKY interaction have interesting properties that are quite distinct from those of the trimers studied pre-

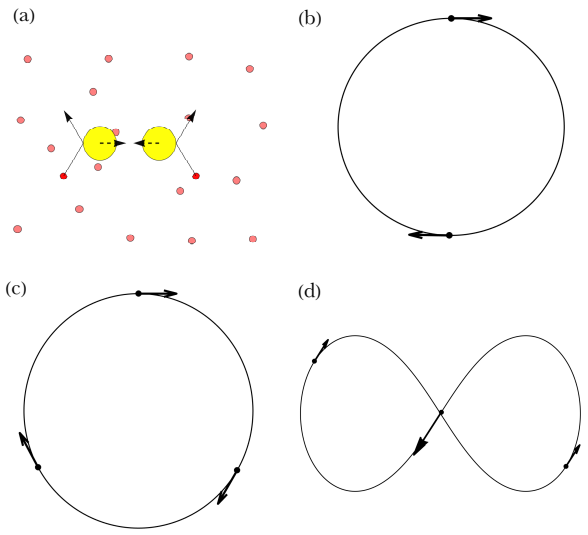

FIG. 1: (a) Schematic of attractive force between bosons (yellow), mediated by the scattering of fermions (red). (b) A two-body orbit. (c) A circular three-body orbit. (d) A figure-eight three-body orbit.

viously. As appropriate for the bound states supported by a long-range attraction, the underlying physics can be best understood in a quasiclassical framework. Below, we apply the quasiclassical quantization using the Gutzwiller trace formula framework. We consider the two simplest periodic orbits of a three-body problem: the circular one and the figure-eight orbit[15] pictured in Fig.1 (c) and (d), respectively. For both orbits the dynamics is locally stable, such that small perturbations remain small at all times.

The figure-eight orbit is an interesting solution to the planar three-body problem in which three equal mass particles travel around a figure-eight curve with time shifts equal to 1/3 of the period, as illustrated in Fig.1(d). It is the simplest periodic orbit in a large family discovered by Moore[15]. Originally it was located numerically using a functional gradient descent procedure described in Sec.IV; its existence was later confirmed by a rigorous analysis[16]. The circular orbits share these properties with the figure-eight orbits.

The analysis of the quantum states associated with these orbits predicts Rydberg-like energy spectra

$$E_n = -C\frac{\alpha^2 m}{4\hbar^2 n^2}, \tag{3}$$

where the prefactor C depends on the orbit geometry; n is an integer taking all positive values $n \geq 1$ for distinguishable particles, and values $n = 1 + 3k$ for identical bosonic particles. The energy spectrum, Eq.(3), is written in the form that facilitates comparison with the conventional Rydberg spectrum, which for two particles of equal masses is given by Eq.(3) with $C = 1$. For the circular-orbit three-body dynamics we find $C = 9$; for the figure-eight orbit we find $C \approx 34$. Comparing to the two-body hydrogenic spectrum given by Eq.(3) with $C = 1$, we see that the three-body states are considerably more stable than the two-body states. Indeed, the binding energy is nearly ten times greater for the circular-orbit three-body states than for the two-body states, whereas for the figure-eight orbit it is more than 30 times greater than the two-body binding energy.

Importantly, a larger energy scale translates into a smaller orbit radius. As discussed below, for realistic α values the spatial extent of hydrogenic two-body states exceeds the Fermi wavelength, i.e. it falls outside the range $2k_F R < 1$ in which the fermion-mediated interaction takes on the $-1/r$ form. In contrast, for three-body states the system parameters can be tuned to push the orbit radius under the $2k_F R < 1$ bound, which guarantees the stability of these states.

Stronger binding for the figure-eight states as compared to the circular-orbit states can be understood in terms of the particles' braiding dynamics illustrated in Fig.2. For the figure-eight orbit the dynamics is such that the three particles come much closer to each other than when they are moving along the circular orbit.

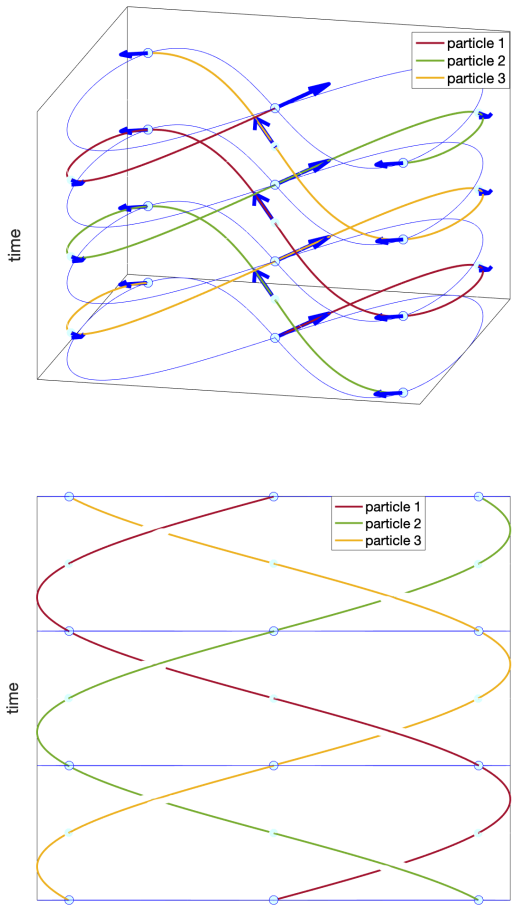

FIG. 2: Braiding dynamics of the figure-eight orbit. The trajectories of the three particles over one full classical period, T, is shown (left). After time $T' = T/3$ the indistinguishable particles return to the original configuration. The explicit braiding of the three states is shown in the lower panel.

II. THE TWO-BODY STATES

For a quantitative estimate we use the parameter values from recent experiment in which the fermion-mediated interaction was observed[12]. The Hamiltonian for bosons embedded in a Fermi sea is of the form

$$H = H_B + H_F + H_{\rm int} \tag{4}$$

In a second-quantized form, the fermion and boson terms read

$$\begin{aligned} H_F &= \int d^3\boldsymbol{r}\phi^\dagger(\boldsymbol{r})\frac{\boldsymbol{p}^2}{2m_F}\phi(\boldsymbol{r}), \\ H_B &= \int d^3\boldsymbol{r}\psi^\dagger(\boldsymbol{r})\left(\frac{\boldsymbol{p}^2}{2m_B} + \frac{g_{BB}}{2}\psi^\dagger(\boldsymbol{r})\psi(\boldsymbol{r})\right)\psi(\boldsymbol{r}), \end{aligned} \tag{5}$$

where $g_{BB} = \frac{4\pi\hbar^2 a_{BB}}{m_B}$ is the intra-species coupling constant, a_{BB} is the corresponding scattering length, and

$m_{B(F)}$ is the boson (fermion) mass. For our purposes, however, the inter-species interaction term is most important:

$$H_{int} = g_{BF}\int d^3\boldsymbol{r}\psi^\dagger(\boldsymbol{r})\phi^\dagger(\boldsymbol{r})\phi(\boldsymbol{r})\psi(\boldsymbol{r}), \quad g_{BF} = \frac{2\pi\hbar^2 a_{BF}}{m_*} \tag{6}$$

with a_{BF} the inter-species scattering length, and $m_* = m_B m_F/(m_B+m_F)$ is the reduced mass. The fermion-mediated interaction can be obtained by integrating out the fermion degrees of freedom. To lowest order in the coupling g_{BF}, this gives an effective bosonic interaction[14]

$$\hat{H}_{int} \approx \frac{1}{2}\int d^3r d^3r' \psi^\dagger(\boldsymbol{r})\psi^\dagger(\boldsymbol{r}')U(\boldsymbol{r}-\boldsymbol{r}')\psi(\boldsymbol{r}')\psi(\boldsymbol{r}) \tag{7}$$

where $U(R)$ is the RKKY interaction potential given in Eq.(1) with the coupling strength

$$3\alpha = \frac{g_{BF}^2 m_F}{\hbar^2(2\pi)^3}, \tag{8}$$

where k_F is the Fermi momentum.

For the system studied in Ref.12, the bosons are ^{133}Cs and the fermions are ^{6}Li. Taking $m_B = 113m_p$ and $m_F = 6m_p$, where m_p is the proton mass, gives the reduced mass $m_* \approx \frac{113\cdot 6}{113+6}m_p \approx 5.7m_p$ and the coupling strength

$$g_{BF} = \frac{2\pi\hbar^2 a_{BF}}{5.7m_p}. \tag{9}$$

For small R, by carrying out the expansion to lowest order in $2k_F R \ll 1$,

$$\frac{\sin 2k_F R - 2k_F R\cos 2k_F R}{R^4} \approx \frac{(2k_F)^3}{3R}, \tag{10}$$

we can write $U(R)$ as a "gravitation" potential

$$U(R) = -\frac{g_{BF}^2 m_F k_F^3}{3\hbar^2\pi^3 R} = -\frac{\alpha}{R}, \quad \alpha = 0.0784\frac{\hbar^2 a_{BF}^2 k_F^3}{m_p}, \tag{11}$$

where we substituted the expression for the interspecies interaction strength g_{BF}, Eq.(9). The power-law character of the interaction and its sign can be understood in terms of the fermionic Casimir force as discussed above.

With this effective interaction, we can analyze bound states for two and three bosonic particles. Two interacting particles are described by the Hamiltonian

$$H = \frac{\boldsymbol{p}_1^2}{2m} + \frac{\boldsymbol{p}_2^2}{2m} + U(\boldsymbol{r}_1 - \boldsymbol{r}_2) \tag{12}$$

where from now on m labels the bosonic mass. The discrete energy spectrum is found readily by separating the center of mass motion, which gives a hydrogenic Rydberg formula with a reduced mass

$$E_n = -\frac{1}{4}\frac{\alpha^2 m}{\hbar^2 n^2}, \quad n = 1,2,3... \tag{13}$$

With this, we estimate the ground state frequency $\nu_1 = \frac{|E_1|}{2\pi\hbar}$ as

$$\begin{aligned}\nu_1 &= \frac{\alpha^2 m}{4\hbar^3(2\pi)} = \frac{133m_p}{8\pi\hbar^3}\left(\frac{0.0784\cdot k_F^3\hbar^2 a_{BF}^2}{m_p}\right)^2 \\ &\approx 1.56\times 10^{-11}\left(\frac{a_{BF}}{a_0}\right)^4\left(\frac{k_F}{k_F^{(0)}}\right)^6 \text{ [Hz]}\end{aligned} \tag{14}$$

where we have chosen to normalize the scattering length a_{BF} and the Fermi wavevector k_F by Bohr's radius a_0 and $k_F^{(0)} \approx \pi\,\mu\text{m}^{-1}$, the value from Ref.12. Choosing $a_{BF} = 100a_0$ and $k_F = 10k_F^{(0)}$, we find from Eq.(14) the value $\nu_1 \approx 1.56$ kHz, or in units of temperature, $h\nu_1/k_B \approx 1.16\cdot 10^{-8}$ K.

Now we must check whether these two-body states are sufficiently tightly bound to fall in the $2k_F R \ll 1$ range of distances, in which the RKKY interaction is of a $1/r$ form. We estimate the typical separation between bosons by taking it to be the Bohr's radius evaluated for a reduced mass value:

$$R_0 = \frac{2\hbar^2}{m\alpha} = \frac{2\cdot a_{BF}^{-2}k_F^{-3}}{133\cdot 0.0784} = 2.2\left(\frac{a_0}{a_{BF}}\right)^2\left(\frac{k_F^{(0)}}{k_F}\right)^3 \text{ [meters]}. \tag{15}$$

Then for the quantity $2k_F R$, which we previously approximated to be small, we have

$$2k_F R_0 = 2\left(\frac{k_F}{k_F^{(0)}}\right)k_F^{(0)}R_0 = 1.61\cdot 10^7\left(\frac{a_0}{a_{BF}}\right)^2\left(\frac{k_F^{(0)}}{k_F}\right)^2. \tag{16}$$

Choosing a realistic value for the interspecies scattering length $a_{BF} = 100a_0$ and $\frac{k_F}{k_F^{(0)}} = 10$ as before, we find $2k_F R_0 \approx 16$. This value is too large to justify the approximation $2k_F R \ll 1$, indicating that in this case the two-body bound states do not occur.

The conditions for confinement can be relaxed by tuning system parameters. Indeed, choosing higher values $a_{BF} = 500a_0$ and $k_F = 20k_F^{(0)}$, we find a fairly large frequency value

$$\nu_1 = 6.24\cdot 10^7 \text{ Hz}, \tag{17}$$

which in units of temperature is $h\nu_1/k_B = 4.6\cdot 10^{-4}$ K. At these values, we also find

$$2k_F R_0 = 0.16, \tag{18}$$

which is justifiably small. However, at present accessing such high values of a_{BF} and k_F may be challenging.

III. THE THREE-BODY STATES

Next, we consider the three-body states and argue that in this case the conditions for reaching bound states become less stringent. The three-body states are described

by the Hamiltonian

$$H(\boldsymbol{r}_i, \boldsymbol{p}_i) = \sum_i \frac{\boldsymbol{p}_i^2}{2m} + \sum_{i \neq i'} U(\boldsymbol{r}_i - \boldsymbol{r}_{i'}), \quad i, i' = 1, 2, 3. \tag{19}$$

The long-range character of the interaction suggests using the quasiclassical method, in which the bound states arise from quantized periodic orbits. However, in contrast to the two-body problem, the three-body problem is non-integrable; as a result, the dynamics is a chaotic in most of the phase space. Yet, islands of stability associated with certain periodic orbits are known to exist, giving rise to families of discrete states. Here we consider such discrete states for the two types of periodic orbits pictured in Fig.1 (c) and (d): the circular orbits and the figure-eight orbits.

The figure-eight orbit is unique up to symmetries of the equations of motion, which include translation, rotation, and rescaling of the $\boldsymbol{r}_i$ and $\boldsymbol{p}_i$ variables

$$\boldsymbol{r}_i \to \frac{1}{\beta}\boldsymbol{r}_i, \quad \boldsymbol{p}_i \to \beta^{1/2}\boldsymbol{p}_i, \quad H \to \beta H \tag{20}$$

(which is a symmetry for the problem with the Newtonian interaction $U(r) = -\alpha/r$). A remarkable property of the figure-eight orbits is that they are linearly stable, which is generally rare for periodic orbits of the three-body problem. The linear stability property was demonstrated in Refs.[17,18] through verifying that all eigenvalues of the stability matrix lie on the unit circle.

Here, we analyze the three-body bound states using the Gutzwiller's semiclassical quantization of non-integrable Hamiltonian systems[19]. The Gutzwiller's approach identifies the contribution to the density of states due to the quantum states associated with periodic orbits, allowing one to separate the discrete states from the chaotic continuum. We apply this approach to the figure-eight orbit, first considering the case where the particles are distinguishable, such that the period of the orbit equals the time it takes for each particle to undergo a full revolution. We then consider the case of indistinguishable particles. In this case, the period is reduced by 1/3, since the particles reach a permuted version of the initial point in phase space, and thus the same quantum state, after a third of the period.

As a quick reminder, the Gutzwiller trace formula approximates the density of states of a non-integrable Hamiltonian system as[19]

$$D(E) = \bar{D}(E) + \mathrm{Re} \sum_p \frac{T_p}{\pi\hbar} \sum_{r=1}^{\infty} A_{p,r} e^{\frac{ir S_p}{\hbar} - \frac{i\sigma_{pr}\pi}{2}} \tag{21}$$

where p sums over all primitive (non-repeated) periodic orbits with energy E, period T_p, action $S_p = \int \boldsymbol{p} \cdot d\boldsymbol{q}$, and r sums over all repetitions of a primitive orbit. Here σ_{pr} is the Maslov index for the r-th repetition of the primitive orbit p, see Ref.20. The amplitude factor $A_{p,r} = |\det(M_p^r - 1)|^{-1/2}$ is a function of the stability, or monodromy, matrix M_p that describes the local flow linearized about the primitive orbit p. The quantity $\bar{D}(E)$ is the average density of states of the system which depends smoothly on energy (the Thomas-Fermi contribution associated with the chaotic states). In our calculations, we will disregard this term because we care only about the oscillatory contribution to the density of states, which arises from the sum over classical periodic orbits. For simplicity, we set the amplitude factor $A_{p,r} = 1$ and also assume the Maslov index to be additive over successive repetitions r of a primitive orbit p; denoting the index for one revolution of the orbit as $\mu \equiv \sigma_{p1}$ we write $\sigma_{pr} = r\mu$. The oscillatory contribution to the density of states is then given by a sum of terms multiplicative in r:

$$\delta D(E) = \mathrm{Re} \sum_p \frac{T_p}{\pi\hbar} \sum_{r=1}^{\infty} \exp\left[ir\left(\frac{S_p}{\hbar} - \frac{\mu\pi}{2}\right)\right]. \tag{22}$$

The validity of the simplifying assumptions that lead to Eq.(22) will be analyzed elsewhere.

We first consider the figure-eight orbits for distinguishable particles. Due to the scaling symmetry of the three-body problem, Eq.(20), there is a continuous family of figure-eight orbits that are equivalent up to a rescaling. If $\boldsymbol{r}(t)$, $\boldsymbol{p}(t)$ is a figure-eight solution with energy E, period T, and action S, then so is

$$\boldsymbol{r}'(t) = \beta^{-1}\boldsymbol{r}(\beta^{3/2}t), \quad \boldsymbol{p}'(t) = \beta^{1/2}\boldsymbol{p}(\beta^{3/2}t) \tag{23}$$

with energy $E' = \beta E$, period $T' = \beta^{-3/2}T$ and action $S' = \beta^{-1/2}S$, for any $\beta > 0$. Since each orbit with energy E can contribute to the density of states only at $D(E)$, our calculation must incorporate the scaling relations into the trace formula. To proceed, we calculate the energy, period, and action of one particular "reference" figure-eight orbit, which we label $\bar{E}$, $\bar{T}$ and $\bar{S}$. The scaling factor β for a figure-eight orbit with energy E, taken relative to an orbit with energy $\bar{E}$, is given by $\beta_E = E/\bar{E}$. Then the action and the period of the rescaled orbit can be written as

$$S_E = \beta_E^{-1/2}\bar{S}, \quad T_E = \beta_E^{-3/2}\bar{T}. \tag{24}$$

We can now write the oscillatory contribution to the density of states from the entire family of figure-eight orbits as a function of E:

$$\delta D(E) = \mathrm{Re}\, \frac{\bar{T}\beta_E^{-3/2}}{\pi\hbar} \sum_{r=1}^{\infty} \exp\left[ir\left(\frac{\bar{S}}{\hbar}\beta_E^{-1/2} - \frac{\mu\pi}{2}\right)\right]. \tag{25}$$

The sum over repetitions r is a geometric series which equals

$$\delta D(E) = \mathrm{Re}\, \frac{\bar{T}\beta_E^{-3/2}}{\pi\hbar} \frac{\exp\left[i\left(\frac{\bar{S}}{\hbar}\beta_E^{-1/2} - \frac{\mu\pi}{2}\right)\right]}{1 - \exp\left[i\left(\frac{\bar{S}}{\hbar}\beta_E^{-1/2} - \frac{\mu\pi}{2}\right)\right]} \tag{26}$$

The poles of Eq.(26) lead to delta functions in the density of states whenever $\frac{\bar{S}}{\hbar}\left(\frac{\bar{E}}{E}\right)^{1/2} - \frac{\mu\pi}{2} = 2\pi n$. Rearranging

this condition, we find the energies E_n of the figure-eight orbit with distinguishable particles, labeled by a quantum number n:

$$E_n = \frac{\bar{E}\bar{S}^2}{4\hbar^2\pi^2(n+\frac{\mu}{4})^2}. \tag{27}$$

Using the numerical method described in Sec.IV, we find $\bar{E} = -1.2935\alpha$ and $\bar{S} = 16.1609(\alpha m)^{1/2}$. The values $\bar{E}$ and $\bar{S}$ depend on the orbit used as an initial condition in the relaxation dynamics. However, their product $\bar{E}\bar{S}^2$ is a universal constant independent of the details of the procedure. Evaluating

$$C = \bar{E}\bar{S}^2/\pi^2 = 34.23..., \tag{28}$$

and setting the Maslov index to its one-body and two-body value $\mu = 4$ (and shifting $n+1 \to n$) yields the result in Eq.(3).

We now consider how Eq.(27) must be modified for the case of indistinguishable particles. This is done by accounting for the permutation symmetry of the three-particle states. Consider a figure-eight orbit with total period T and action S, where the particles start at the initial point $(\boldsymbol{r}, \boldsymbol{p})$ in phase space. Then after a time $T/3$, the particles reach a permuted version of the initial phase space point, $(P\boldsymbol{r}, P\boldsymbol{p})$, where P is the operator corresponding to the permutation (123). Since the particles are indistinguishable, the system has reached a quantum state which is identical to the initial state, and we can think of $T/3$ as the new period of the system. Then the action of the system becomes $S/3$. Since the Maslov index for the modified orbit is one third of the value for the original orbit, we replace $\bar{S}$ with $\bar{S}/3$ and μ with $\mu/3$ in Eq.(27). This yields the spectrum in Eq.(3) with n taking values 1, 4, 7, 10, and so on.

Another way to arrive at this result is to consider the ground state for distinguishable particles for which the wavefunction is nodeless and is therefore identical to that for the ground state of bosonic particles. The number of nodes for the excited states, from permutation symmetry, must equal $3k$ for some positive integer k value, which leads to Eq.(3) with $n = 1+3k$ as above.

Our analysis of the figure-eight orbit can be easily extended to circular orbits, where three particles travel along a circular path with fixed time shifts equal to 1/3 of the period [Fig.1 (c)]. This orbit is known to be stable[15], and its permutation symmetry is identical to that of the figure-eight orbit. In the case of distinguishable particles, we need only calculate $\bar{E}$ and $\bar{S}$ and plug these values into Eq.(27). In the case of indistinguishable particles, we must also consider how the period of the orbit and therefore $\bar{S}$ are modified due to permutation symmetry. For the case of distinguishable particles, we find values

$$\bar{E} = -\frac{3^{1/2}\alpha}{4}, \quad \bar{S} = 2\pi(3^{3/2}\alpha m)^{1/2}, \tag{29}$$

which gives $E_n = -9\alpha^2 m/4\hbar^2(n+\frac{\mu}{4})^2$, which is nothing but Eq.(3) with $C = 9$. For identical bosonic particles, we account for permutation symmetry as above, noting that the ground state, which is nodeless, can be populated by three bosons. This again yields Eq.(3) with n replaced with $1+3k$.

Because of the inverse relation between energy and distance, larger binding energies translate into smaller spatial scales for the orbits. Starting from the relation in Eq.16 and rescaling it by the factors of $C = 9$ and $C \approx 34$ for the two types of orbits gives

$$2k_F R_0 = \frac{1}{C} 1.61 \cdot 10^7 \left(\frac{a_0}{a_{BF}}\right)^2 \left(\frac{k_F^{(0)}}{k_F}\right)^2. \tag{30}$$

Choosing the same values for the interspecies scattering length and the Fermi momentum as above, $a_{BF} = 100a_0$ and $\frac{k_F}{k_F^{(0)}} = 10$ as before, we find $2k_F R_0 \lesssim 1$ for the circular orbit and $2k_F R_0 \ll 1$ for the figure-eight orbit. The small values of $2k_F R_0$ justify our $U(R) \sim -1/R$ approximation. Tighter confinement of the three-body states as compared to the two-body states indicates their higher stability.

We attribute the higher stability of the figure-eight states, as compared to that of circular orbits, to the "intertwining" character of the figure-eight dynamics that brings particles much closer to each other than for other types of orbits. This property, as well as other interesting properties such as the braiding character of the dynamics, illustrated in Fig.2, makes these states particularly well-suited for exploring non-Efimov trimer states.

More generally, our analysis can be applied to any orbit of the n-body problem, since the derivation of Eq.(27) depends only on the scaling properties of the system, and not on the number of particles. Interestingly, the figure-eight orbit is known to exist in the n-body problem for all odd $n \geq 3$[24], and one could thus use the same method to calculate the spectra of n-body bound states of the figure-eight orbit. Quantum states associated with these orbits, if realized in experiment, can provide a unique opportunity to demonstrate braiding that results directly from unitary quantum evolution that does not depend on external driving.

We are grateful to Alexander Turbiner, Chang Chin and Vladan Vuletic for useful discussions.

[1] V. Efimov, Energy levels arising from resonant two-body forces in a three-body system, *Phys. Lett. B* **33** 563-564 (1970).

[2] P. Naidon and S. Endo, Efimov physics: a review, *Rep.*

Prog. Phys. **80**, 056001 (2017).
[3] A. LeClair, J. Maria Román and G. Sierra, Russian doll renormalization group and superconductivity *Phys. Rev. B* **69**, 020505 (2004).
[4] P. F. Bedaque, H.-W. Hammer and U. van Kolck, Renormalization of the three-body system with short-range interactions *Phys. Rev. Lett.* **82**, 463 (1999).
[5] S. D. Glazek and K. G. Wilson Limit cycles in quantum theories *Phys. Rev. Lett.* **89**, 230401 (2002).
[6] B. Huang, L. A. Sidorenkov, R. Grimm and J. M. Hutson, Observation of the second triatomic resonance in Efimovs scenario, *Phys. Rev. Lett.* **112**, 190401 (2014).
[7] S.-K. Tung, K. Jiménez-Garca, J. Johansen, C. V. Parker and C. Chin, Geometric scaling of Efimov states in a ^6Li-^{133}Cs mixture, *Phys. Rev. Lett.* **113**, 240402 (2014).
[8] R. Pires, J. Ulmanis, S. Hafner, M. Repp, A. Arias, E. D. Kuhnle and M. Weidemuller, Observation of Efimov resonances in a mixture with extreme mass imbalance *Phys. Rev. Lett.* **112**, 250404 (2014).
[9] M. A. Ruderman and C. Kittel, Phys. Rev. 96, 99 (1954).
[10] T. Kasuya, Prog. Theor. Phys. 16, 45 (1956).
[11] K. Yosida, Phys. Rev. 106, 893 (1957).
[12] B. J. DeSalvo, K. Patel, G. Cai and C. Chin Observation of fermion-mediated interactions between bosonic atoms *Nature* **568**, 61-64 (2019).
[13] D. Zhabinskaya, J. M. Kinder, and E. J. Mele, *Phys. Rev. A* **78**, 060103(R) (2008).
[14] S. De and I. B. Spielman, Appl. Phys. B. 114, 527 (2014).
[15] C. Moore, Phys. Rev. Lett. 70, 3675 (1993).
[16] A. Chenciner and R. Montgomery, Annals of Mathematics. Second Series 152, 881 (2000).
[17] T. Kapela and C. Simó, Nonlinearity 20, 1241 (2007).
[18] G. E. Roberts, Ergodic Theory and Dynamical Systems 27, 19471963 (2007).
[19] M. C. Gutzwiller, J. Math. Phys. 12, 343 (1971).
[20] S. C. Creagh, J. M. Robbins, and R. G. Littlejohn, Phys. Rev. A 42, 1907 (1990).
[21] S. C. Creagh and R. G. Littlejohn, Phys. Rev. A 44, 836 (1991).
[22] S. C. Creagh and R. G. Littlejohn, J. Phys. A: Math. and Gen. 25, 1643 (1992).
[23] M. Brack and S. R. Jain, Phys. Rev. A 51, 3462 (1995).
[24] C. Simó, New Families of Solutions in N-Body Problems, In: C. Casacuberta, R. M. Miró-Roig, J. Verdera, S. Xambó-Descamps (eds) European Congress of Mathematics. Progress in Mathematics, vol 201. Birkhauser, Basel

IV. APPENDIX: ORBIT RELAXATION

The Gutzwiller Trace formula relies on quantities such as the action, energy, and stability matrix eigenvalues of the periodic orbits of a dynamical system. To extract these quantities for a periodic orbit of the planar three-body problem, we require a numerical solution of the orbit, since in general no closed-form solution exists. Here, we describe a numerical "relaxation" procedure for locating periodic orbits of the planar n-body problem in phase space, based off of work by Moore[15]. The procedure is a functional gradient descent that minimizes the action functional $S[\boldsymbol{r}_1(t)\dots\boldsymbol{r}_n(t)]$, where $\boldsymbol{r}_1(t)\dots\boldsymbol{r}_n(t)$ are the trajectories of n point particles each with mass m. We start by choosing fictional periodic orbits for each particle. To each orbit we apply a functional differential equation in fictional time τ:

$$\frac{d\boldsymbol{r}_i(t)}{d\tau} = \gamma\left(m\frac{d^2\boldsymbol{r}_i(t)}{dt^2} - \sum_{j\neq i}\boldsymbol{F}_{ij}(t)\right), \quad i,j = 1...n, \tag{31}$$

where $\boldsymbol{F}_{ij}(t) = -\alpha\frac{\boldsymbol{r}_i(t)-\boldsymbol{r}_j(t)}{|\boldsymbol{r}_i(t)-\boldsymbol{r}_j(t)|^3}$ is the force from particle j acting on particle i at time t, and γ is a parameter that controls the descent rate. Once $d\boldsymbol{r}_i(t)/d\tau = 0$ for each $\boldsymbol{r}_i(t)$, the procedure has converged upon solutions to the equations of motion, since $md^2\boldsymbol{r}_i(t)/dt^2 = \sum_{j\neq i}\boldsymbol{F}_{ij}(t)$. The right hand side of Eq.(31) can be rewritten as $-\frac{1}{m}\nabla S[\boldsymbol{r}_1(t)\dots\boldsymbol{r}_n(t)]$, where ∇S is the functional gradient or the variational derivative of S. The procedure is then a functional gradient descent which decreases the action at each step, until the procedure converges and the action reaches a local minimum. As described by Moore, applying the procedure leads to a few possibilities, one of which is the convergence to a genuine periodic orbit of the system. In this case, the nature of the solution is determined by the topology of the initial orbit. In particular, if we plot the orbits of n bodies in the plane against time, the orbits draw out a braid of n strands in three-dimensional space-time. This braid is a topological classification of the motion which remains constant over the course of relaxation, as long as no collisions between particles occur. Other possibilities of applying relxation are that two or more of the particles collide, causing a change in topology, or that one or more of the particles escapes to infinity. Escape occurs when the braid is separable, i.e when the strands can be separated into two or more isolated subsets. For $1/r$ potentials, certain braids always lead to collision, forbidding any solution from having that braid-type (the same is not true of "strong-force" $1/r^2$ potentials, where there is a solution for every braid). The reasons for this are discussed in detail by Moore and will not be the subject of this description. In summary, the relaxation method is a relatively fast, accurate way of locating solutions to the planar n-body problem of a desired topology, allowing us to obtain the quantities necessary for the Gutzwiller Trace formula. For instance, we can easily locate the three-body figure-eight solution by choosing initial trajectories of the form:

$$\boldsymbol{r}_1(t) = \begin{pmatrix}\sin(t-\frac{2\pi}{3})\\ \sin(t-\frac{2\pi}{3})\cos(t-\frac{2\pi}{3})\end{pmatrix} \tag{32}$$

$$\boldsymbol{r}_2(t) = \begin{pmatrix}\sin(t)\\ \sin(t)\cos(t)\end{pmatrix} \tag{33}$$

$$\boldsymbol{r}_3(t) = \begin{pmatrix}\sin(t+\frac{2\pi}{3})\\ \sin(t+\frac{2\pi}{3})\cos(t+\frac{2\pi}{3})\end{pmatrix} \tag{34}$$

for $0 \leq t \leq 2\pi$, where the trajectories are overlapping figure-eight orbits with period 2π, phase-shifted from one another by $\frac{2\pi}{3}$. Applying the relaxation method converges to the true figure-eight solution with period 2π and energy -1.2935 (for $\alpha = 1, m = 1$).